AD-A178 517 CARBON FIBRE COMPOSITE COUPONS - STATIC AND FATIGUE BEHAVIOUR AFTER IMPACT DAMAGE(U) AERONAUTICAL RESEARCH LABS MELBOURNE (AUSTRALIA) G CLARK ET AL. AUG 86 1/1

UNCLASSIFIED ARL/STRUC-R-422 F/G 11/4 NL

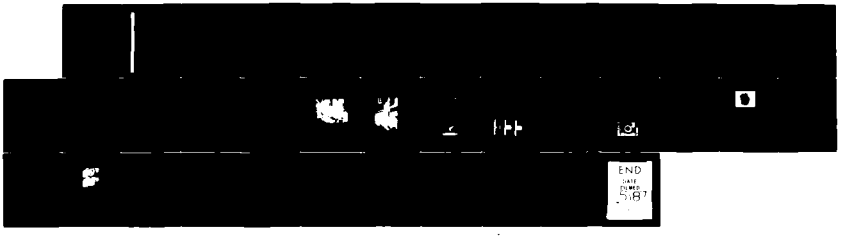

END
DATE FILMED
5-87

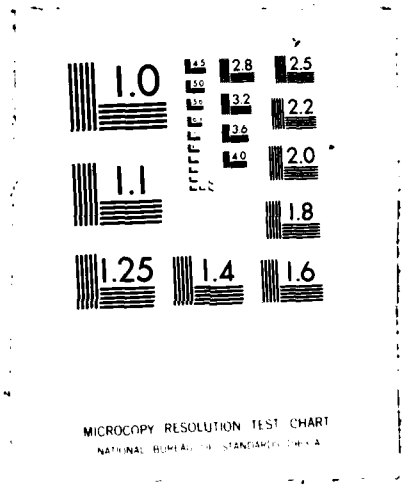
1.0
1.1
1.25
1.4
1.6
2.8
3.2
3.6
4.0
2.5
2.2
2.0
1.8
MICROCOPY RESOLUTION TEST CHART

ARL-STRUC-R-422

AR-004-495

DEPARTMENT OF DEFENCE

DEFENCE SCIENCE AND TECHNOLOGY ORGANISATION

AERONAUTICAL RESEARCH LABORATORIES

MELBOURNE, VICTORIA

STRUCTURES REPORT 422

CARBON FIBRE COMPOSITE COUPONS - STATIC AND FATIGUE BEHAVIOUR AFTER IMPACT DAMAGE

by

G. CLARK and T.J. VAN BLARICUM

COPY No

AUGUST 1986

AR-004-495

DEPARTMENT OF DEFENCE
DEFENCE SCIENCE AND TECHNOLOGY ORGANISATION
AERONAUTICAL RESEARCH LABORATORIES

Structures Report 422

CARBON FIBRE COMPOSITE COUPONS - STATIC AND FATIGUE BEHAVIOUR AFTER IMPACT DAMAGE

by

G. CLARK and T.J. VAN BLARICUM

SUMMARY

This report describes some results from an experimental program involving the determination of static and fatigue properties of relatively thick (3 to 7 mm) carbon fibre composite laminates which had been subjected to various levels of impact damage. The development of suitable compression testing procedures is described, as is the use of shadow Moire interference techniques for monitoring the development of delamination damage during fatigue tests.

POSTAL ADDRESS: Director, Aeronautical Research Laboratories,
P.O. Box 4331, Melbourne, Victoria, 3001, Australia.

CONTENTS

GLOSSARY OF TERMS

σ_c Critical buckling stress

E_x Elastic modulus of laminate in 0^o direction

ν Poisson's ratio (inplane) of laminate

L Length of specimen gauge area

t Laminate thickness

1. INTRODUCTION

Research currently underway in Structures Division of the Aeronautical Research Laboratories (ARL) includes the investigation of damage tolerance of carbon-fibre composite (CFC) laminates in structural applications. One part of this program involves the fatigue testing of an impact-damaged composite/metal box-beam structure representative of an aircraft inner wing torque box (Fig. 1). A second program involves testing of CFC coupons, in support of the box-beam structural test, and also as a means of investigating more directly the damage tolerance of CFC material used in various applications. The coupon test program will investigate the following:

a. Static compression behaviour, with and without impact damage.

b. Tension and in-plane shear performance of undamaged laminates.

c. Moisture absorption properties, in support of environmental conditioning programs.

d. Fatigue of impact-damaged coupons, to determine the conditions under which delaminations will grow.

e. Effects of variable amplitude loading, particularly the effects of spectrum truncation.

f. Effects of combined variable-amplitude loading and environmental cycling, in order to determine the extent to which the environmental cycle and its rate of application affect fatigue lives.

This report describes results and details of the developmental work conducted under programs (a) and (d) above.

2. EXPERIMENTAL

2.1. Materials

The CFC material used in the test program is designated XAS-914C; this is a UK-manufactured laminate which forms part of the ARL box beam, in a $[\pm 45/0_2]_{7S}$ lay-up. ARL has also manufactured the same laminate from pre-impregnated sheet, as 56-ply $[\pm 45/0_2]_{7S}$; this was used in the present tests together with 24-ply $[\pm 45/0_2]_{3S}$ CFC sheet of UK manufacture.

2.2 Specimen Configuration

The tests described below were carried out on 24-ply and 56-ply coupons with a size of 220 x 72 mm, and a gauge area of 80 x 72 mm. Coupon thicknesses were approximately 3 mm and 7 mm respectively. The moisture content of 56-ply coupons was determined (by drying out) to be approximately 0.2% by weight, that of the 24-ply laminates being typically 0.5%. It was decided to grip the specimens directly rather than use bonded end tabs which are often recommended in standard test procedures, eg. reference [1]; the basis for this decision was that differential thermal contraction of the specimens and tabs during cooling from the bonding temperature can produce unacceptably high levels of tension in the through-thickness direction. The magnitude of this stress can be sufficient to cause specimen delamination [2]. A further consideration was that the use of end tabs introduces another potential source of specimen misalignment. The approach eventually adopted was to grip the specimen between finely serrated En25 steel jaws, using an open weave abrasive impregnated cloth sheet ('Screenback') as an interlayer. A grip pressure of approximately 270 MPa led to no indications of slippage in static tests. A small amount of fretting was observed in fatigue tests but this was limited to a region near the edge of the gripped area, and did not become a significant problem even after 3×10^6 cycles. The gauge area of each specimen was spray-painted white on one face, to aid in damage monitoring (see Section 2.5).

2.3 Strain Gauging

Strain gauging of composites involves a number of problems not normally experienced with metals, the major one being that of ensuring that the adhesives used do not deteriorate under exposure to the hot humid conditions required for specimen conditioning and testing. In the current tests, a room-temperature curing anaerobic adhesive (M-Bond 200) was used to attach 6 mm resistance strain gauges. In general, the gauges performed reliably in static tests; in fatigue, however, gauge or adhesive failure invariably occurred long before specimen failure, indicating that the high cyclic strain ranges (between 3 000 and 6 500 microstrain) which may be applied for between 10^4 and 10^7 cycles in fatigue testing of composites can be a severe test of strain gauging techniques. Gauge lives of less than 50 000 cycles at 6 500 microstrain were observed and, as a result, the influence of surface preparation and adhesive selection on gauge performance is currently under investigation. The use of fatigue-rated extensometers is also being examined.

The use of strain gauges for an initial strain survey is common in structural testing (eg. the box-beam tests described earlier), and it should be noted that as a result of anisotropy in the composite sheet, some gauge orientations and laminate lay-ups can provide erroneous strain readings [3]. An extreme case is that of a unidirectional lay-up in which both the fibres and strain gauges are normal to the maximum applied stress; where the gauge will provide strain readings which may be of opposite sign to the true strain in the laminate. This problem arises in situations where strain gauges perceive high strains normal to their length as a result of laminate anisotropy. The effect of this transverse strain on the gauge output can mask the effect of a small strain change along the length of the gauge. Consequently, the magnitude of this effect is currently being examined in a range of laminate lay-ups. In the tests described below, strain gauge output was recorded through conventional strain gauge bridge amplifiers, except in a small number of cases where four gauges were attached to the specimen; in these cases a constant current DC power supply programmed by an HP85 computer was used, and gauge output voltages were read directly by a nanovoltmeter and recorded automatically by the computer system.

2.4 Impact Damage

Figure 2 shows the physical arrangement of the system used to introduce impact damage. The specimens were clamped tightly between two sections of 76 x 76 mm rectangular hollow steel section, and impacted on the unpainted face by a falling mass of either 0.5 or 1 kg, at the nose of which was a 12.7 mm diameter steel ball. A laser timing system was used to monitor impact and rebound velocities just above the specimen surface; these values were then used to derive a measure of incident and absorbed energies. Trials of the system indicated that the rig provided free-fall conditions for the indentor, within measurement error. The maximum energy available in the system was 20 J.

Typical impact energy levels (ie. beteen 3 to 20 J) expected in service are often represented by the case of a hammer being dropped from working height. In the present tests, a range of energy values was chosen. For the 24-ply coupons the values were from 2 to 6.5 J, the maximum energy level used being determined by the development of cracking in the rear face of the coupon, while the minimum energy was chosen to produce delamination damage which was barely detectable using ultrasonic inspection. The 56-ply coupons were subjected to incident impact energies between 4 and 11 J, with no evidence of rear face damage.

2.5 Damage Size Monitoring

2.5.1 Ultrasonic techniques

Monitoring the size of delamination damage in carbon fibre composites is significantly more difficult than monitoring crack length in metals. Procedures used include X-ray tracking of delamination growth after the injection of a radio-opaque image-enhancing dye [4], ultrasonic measurement of delamination size, and thermography [5]. The use of dyes was regarded as undesirable, in view of the possibility of introducing unwanted environmental effects, and the procedure adopted here [6] was based on ultrasonic scanning of the specimen. Specimens were examined in a conventional immersion C-scanning frame, which was modified to incorporate a thickness gauge in order to obtain data concerning the depth of the damage below the coupon surface, together with its location in the laminate. Data were recorded in a microcomputer system and were then available for display or further analysis. This system is capable of examining any cross-section through the coupon, and displaying the defect location. By alternately scanning from both sides of the sheet, a detailed image of the damage envelope could be built up, as is illustrated in Fig. 3 for a 56-ply impact-damaged laminate. This method was used to determine the condition of the undamaged coupons and, after impact, to determine the extent and location of the impact damage.

2.5.2 Shadow Moire technique

The three-axis ultrasonic scanning system could not be used while coupons were under test, and an alternative procedure based on the Shadow Moire technique [7] was used for damage monitoring during the course of fatigue and static tests. This technique uses an optical grid, with typically 10 to 20 lines per mm, positioned close to the white-painted specimen surface. The grid is illuminated at 45° to the normal and the resultant shadow of the grid on he specimen is viewed through the grid itself, providing interference fringe representation of any variation in the distance from grid to specimen. The technique is capable of measuring out-of-plane displacements resulting from buckling or distortion with a sensitivity of typically 0.15 mm/fringe.

2.5.3 Compliance measurement

A third approach to damage size monitoring, used during fatigue tests, consisted of monitoring the local compliance of the area near the delamination using extensometers. A high-speed data recording system made it possible to measure compliance without interruption of the fatigue test; however at best this technique is only capable of providing an indication that damage growth is occurring.

2.6 Compression Testing Rig Development

A major problem in the testing of composites is the provision of suitable constraint conditions during compression testing [8]. Constraining the area of the specimen containing damage is unacceptable since out-of-plane movement of the plies adjacent to the delamination must be permitted if a realistic stress distribution is to be achieved. Fully constraining the specimen edges, which can be initiation sites for delaminations and other damage processes in undamaged coupons, is also unacceptable. At the same time, it is desirable to test impact damaged coupons which are large enough to provide infinite-sheet conditions for damage growth; however, this leads to the possibility of gross specimen buckling. In itself, buckling is not necessarily unacceptable, since it is often a failure mode in the aircraft structural applications of interest. However, the design of compression testing fixtures clearly requires some consideration of the extent of the antibuckling measures to be introduced. Testing machine alignment is critical; simple beam calculations indicate that for the specimen sizes used, grip-to-grip out-of-plane misalignment of 0.2 mm would result in maximum uniform bending strains of approximately 200 microstrain. Therefore, alignment of better than 0.08 mm was maintained for all of the work described below.

Several antibuckling restraint systems were investigated and used in the course of this test program. A typical example (shown in Fig. 4), was based on an original design of Sarma Avva [9] in which rollers were clamped against the specimen, some distance in from the edges. These rollers, however, were believed likely to introduce local stress concentrations at their ends if any machine misalignment existed. An ARL modification replaced the roller system with PTFE pads supporting the specimen gauge area around its full perimeter, with the exception of two cutouts (remote form the central damaged region) to allow strain gauges to be attached. The performance of this modified rig was evaluated using a dummy strain-gauged aluminium alloy specimen. Strain surveys indicated unacceptable strain concentrations of up to 450 microstrain (Fig. 5), when the specimen was clamped in the hydraulic grips of the testing machine at zero load. These strains resulted from concentration of the effect of residual machine misalignment, and it was concluded that rig designs based on clamping large rigid plates onto the whole of the specimen gauge area would inevitably result in similar strain concentration problems. A compression rig was therefore developed incorporating features which avoided these difficulties.

The basic ARL-designed rig consists of pairs of En25 steel plates, clamped against the grip area of the specimen; the plates (Fig. 6) have fine serrations on the grip face which assist shear transfer of load to the specimen via an intermediate layer of abrasive coated cloth. Each plate has two integral columns, which serve as support for a variety of antibuckling restraints.

Three types of restraints, shown in Fig. 6 were used; studs (four per plate) which could be screwed up against the specimen surface, crossbars which linked the columns of each plate and contacted the specimen surface across most of its width, and crossbars supporting thick metal pads in the centre of the gauge area. All surfaces in contact with the specimen were PTFE coated. The specimen was assembled into the plate assembly prior to insertion in the hydraulic grips of a 250 kN Instron servohydraulic testing machine. After alignment of the specimen, final adjustment of the antibuckling restraints was carried out with the assembly gripped at the required clamping pressure and under zero axial load. This system has performed satisfactorily to date and larger versions are now in use for other test series.

3. *TEST PROCEDURE, RESULTS AND DISCUSSION*

3.1 56-ply Static Testing

The thicker (56-ply) coupons of the size used did not present a major problem in terms of buckling behaviour. For undamaged laminate the critical stresses (with clamped ends and an unsupported gauge length for Euler buckling, and with clamped ends and simply-supported edges for plate buckling respectively [10]) were estimated from

$$\sigma_c = 4\pi^2 E/[12(L/t)^2] \quad (1)$$

and

$$\sigma_c = 5.5E(t/L)^2/(1-\nu^2) \quad (2)$$

as 2 540 MPa and 8 490 MPa. Values of E = 72.8 GPa and ν = 0.7 were derived from stress-strain data for 24-ply compression specimens. In view of the anticipated compression failure stresses of less than 1 000 MPa, these values indicated that failure by gross buckling should be unlikely. The shadow Moire system was used on specimens supported by studs (Fig. 6a) and crossbars (Fig. 6b) confirming that restraint was unnecessary in the 56-ply tests. Later tests were conducted without any restraint.

Damaged and undamaged specimens were loaded in compression using displacement control, at a strain rate of approximately 3×10^{-5} sec^{-1}, and in addition to a continuous record of load and strain, a record of the Moire fringe pattern was obtained at intervals up to specimen failure.

The results, shown in Fig. 7, indicated that impact damage reduced the residual compressive strength to 47% of the undamaged value (879 MPa), as the delamination area (measured ultrasonically) increased. This result supports data obtained by Cantwell and Morton [11] who reported a reduction to 40% of undamaged strength in eight-ply XAS-914C specimens, and Demuts et al. [12] who noted a similar reduction (to approximately 42%) for a variety of graphite-epoxy systems. The scatter (shown in Fig. 7) in the 56-ply strength versus delamination area is considerable, but re-plotting the residual strength values against both incident and absorbed energy (Fig. 8) shows that the relationship between strength and absorbed energy exhibits much less scatter. The relationship between strength and incident energy however, still displays a high level of scatter, as might be expected since the incident energy necessarily includes significant (and variable) energy losses to the specimen support rig. The form of results in Fig. 8 suggests that residual strength decreases with increasing absorbed impact energy, apparently reaching a minimum value for energies over 6.5 J.

Further examination of individual specimen records showed that the difference between the scatter of the results in Figs 7 and 8 was caused by a small number of specimens in which large absorbed impact energies were recorded. These produced low residual strengths, while ultrasonic examination showed that these specimens contained relatively small areas of delamination. The presence of two distinct types of specimen behaviour is illustrated in Fig. 9. The greater absorbed energy (by approximately 2 J) recorded for one group appears to have been used to produce damage in a form which could not be detected ultrasonically, since a reduction in specimen strength is still observed. Energy losses in the impact system would not explain these observed strength reductions.

Definition of delamination size in 56-ply coupons using the shadow Moire technique was unsatisfactory; the best results achievable (Fig. 10) simply indicated a significant out-of-plane distortion in the region of damage. As illustrated earlier in Fig. 2, ultrasonic examination of these coupons from both sides had revealed that the delamination damage was localised in a region near the mid-plane of the specimen; this would lead to poor definition of the delamination area at the surface and is consistent with the observed inability of the Moire system to define delamination size in these specimens.

The results shown in Fig. 8 also confirmed that, at these loads, the antibuckling restraint system did not influence the results significantly for this specimen size and thickness.

3.2 56-ply Fatigue Testing

In order to determine whether or not significant damage growth occurs in fatigue, specimens containing delaminations of approximately 1 700 mm^2 or with smaller (200 to 300 mm^2) damage were subjected to zero-to-compression fatigue loading at 5 to 10 Hz. Each test commenced with 10^6 cycles at 200 kN, representing approximately 68% of the static failure load expected on the basis of the absorbed energy/residual strength curve in Fig. 8. If the shadow Moire system revealed no significant change in out-of-plane displacement (ie. no apparent damage growth) after 10^6 cycles, the load range was increased to 225 kN, then to 250 kN and finally to 275 kN, in each case for 10^6 cycles (or failure). Failure stress ranges are indicated in Fig. 11, relative to the "static" residual strength data of Fig. 8, and lie between 78% and 95% of the static residual strength. Apart from indicating that fatigue loading can produce failures at stresses less than the static strength level, the results showed a wide range of lives for nominally identical initial damage and fatigue test conditions (eg. 900, 97 730 and 769 290 cycles all obtained under peak stresses of 430 to 460 MPa). However, these are results from a limited number of tests and further investigation of these effects will entail the testing of larger numbers of specimens.

3.3 24-ply Static Testing

Tests using 24-ply coupons were complicated by the need to restrain the gauges area from gross buckling. Figure 12 indicates the different support systems investigated for undamaged coupons. These ranged from studs, 0.1 mm clear of the surface, to arrangements which provided high levels of restraint at the coupon surface. A small number of tests was also conducted using very short (20 mm) gauge length coupons, with no restraint. Clearly, the level of restraint influences the results, in that the high levels of restraint resulted in an undamaged strength (900 MPa) almost double that observed when only studs were used (500 MPa). The short gauge length coupons also gave results close to 900 MPa, supporting the view that this value is close to the true compression failure stress. Use of the shadow Moire system (Fig. 13) and extensometers confirmed that buckling was taking place at about 500 MPa stress for lightly restrained specimens. It was noted that although this is substantially lower than the theoretical plate buckling stress for a 24-ply

column with simply-supported edges and clamped ends (330 MPa from equation 2), such behaviour is not surprising, since perfect specimen alignment can never be achieved.

As a result of the above tests on undamaged coupons, impact-damaged specimens were tested using the arrangement shown in Fig. 6c, the support pads containing holes to permit out-of-plane movement of the material above the delamination. Figures 14 and 15 show the residual static compression strengths achieved. the strength-incident energy curve in Fig. 15 displays a distinct threshold at approximately 2.7 J, making it difficult to use a knowledge of incident impact energy to predict strength losses in service. The variation of strength with absorbed energy, however, would be more convenient from this point of view, except for the fact that absorbed energy is usually impossible to determine in a service environment. Figure 14 shows a clear relationship between the total delamination area (measured near the back surface) and compression strength, and is regarded as a potentially useful curve for relating damage observed to expected changes in mechanical properties.

The scatter in the strength versus delamination area relationship in the 24-ply tests (Fig. 14) is considerably less than was seen in the 56-ply coupons (Fig. 7). the relationship between delamination area and energy absorbed (Fig. 16) showed that, in a majority of cases, consistent behaviour was observed without the apparent intrusion of the other energy-absorbing damage mode which was observed in the 56-ply coupons. However, an isolated results at 3.75 J absorbed energy does show an unusually small area of delamination, suggesting that bimodal behaviour may also occur in 24-ply laminates.

In the 24-ply case, a typical ultrasonic cross-section (Fig. 17) shows that damage development occurs much nearer to the back face of the specimen than was seen in the 56-ply coupons. The envelope of delamination damage is a cone, with the largest extent of delamination nearest to the back face. This observation is consistent with work by Cantwell and Morton [11], who showed that as laminate thickness increased (without changing the support system), damage commenced closer to the upper surface of the coupon.

3.4 24-ply Fatigue Testing

A number of constant-amplitude compression fatigue tests were carried out on 24-ply $[\pm 45/0_2]_{3S}$ coupons containing impact damage. These coupons were identical to those used in the static testing reported above and the same loading rig was used. However, in some cases crossbar-type restraints were used instead of the pad restraint system, in order to permit the use of Moire grids and extensometers. This reduction in constraint was considered acceptable because the damage present in the specimens was such that the stress levels necessary during testing would be less than those required for the undamaged specimens (which had been used to establish the constraint conditions). Fatigue testing was carried out at frequencies between 10 Hz and 15 Hz. Compliance determinations made at the impact damage site during the course of the test clearly indicated damage growth as shown in Fig. 18(a). It should be noted that the strains presented here are local strains, not those experienced by the specimen remote from the damage.

Typical Moire fringe results are illustrated in Fig. 18(b). In the example shown, the out-of-plane displacements on the back face of the specimen were seen to have increased considerably after 50 000 cycles of fatigue. While the Moire results could not provide a measure of the absolute size of the delamination area, they were used to track its growth by plotting, at various stages during the test, a profile of the Moire fringe pattern for a cross section of interest, as shown in Fig. 18(c). These profiles indicate the change in out-of-plane displacement. Selection of a suitable fringe (usually the first-order fringe near the perimeter of the delamination), provides a means of tracking growth of the delamination where, as shown in Fig. 18(d), the proportional increase in fringe system size is given as a function of the number of fatigue cycles. This factor could then be applied to the original ultrasonically-determined delamination size, as shown in Fig. 19.

The remote compressive strain range under which delaminations were seen to grow was as low as 3 200 microstrain. Progressive growth of delamination area from an original size of 430 mm^2 at intervals of 12 500 cycles is shown in Fig. 19. Failure occurred at approximately 90 000 cycles under zero-to-compression fatigue with a peak compressive stress of 286 MPa, i.e. 77% of the expected static failure stress. A similar result was obtained for a coupon with a 500 mm^2 delamination area tested at a lower peak stress, in this case representing 62% of expected static failure stress. In the latter case, delamination growth and failure occurred at only 26% of the undamaged failure stress.

These results indicated that growth of delaminations is possible at stresses much lower than those at which static failure would be expected to occur, and draw attention to the question of the nature of the failure process e.g. does failure occur simply as a result of a single delamination growing to a size which produces static failure? The present tests apparently indicate an asymptotic static failure curve. Assuming that this form (or a gradual reduction in static failure stress) is preserved for high values of delamination area, extremely large delaminations would then be required to produce failure at the fatigue stresses used here. Such large delaminations cannot occur in the coupon sizes tested, indicating that simple growth of delamination area is not the only kind of fatigue damage occurring. Note however, that the form of the static failure curve is critical, and this aspect clearly requires further investigation.

4. CONCLUSIONS

This work has involved the development and introduction of a number of techniques for static and fatigue testing of carbon fibre composites in the critical compression loading mode. Techniques have been developed to overcome the problems associated with buckling of coupons during static and fatigue testing. The use of a shadow-Moire technique for monitoring delamination growth has been demonstrated for 24-ply coupons and the same technique was used to assist with development of antibuckling restraints.

A substantial loss of compression strength with increasing delamination size was observed for both 24-ply and 56-ply impact-damaged laminates, and fatigue failures of impact-damaged coupons was observed for zero-to-compression cycling with peak stresses substantially lower than the residual static compression strength associated with that size of initial damage.

While the loss of compression strength in impact-damaged 24-ply laminates generally correlated well with both delamination area and the energy absorbed during impact, results on 56-ply laminates showed anomalous behaviour; in this case the correlation with absorbed energy and delamination area revealed that in some cases an effective form of damage was being produced (i.e. strength was reduced) while this damage was not reflected in the size of the delamination observed.

5. ACKNOWLEDGEMENTS

The authors would like to acknowledge the contribution to this work of T. Preuss and B. Lawrie of Aeronautical Research Laboratories.

6. REFERENCES

1. American Society for Testing and Evaluation. Standard Test Method for Tensile Properties of Fiber-Resin Composites. Philadelphia, PA: American Society for Testing and Materials, D3039-76: 1976.

2. Broughton, W. Aeronautical Research Laboratories, Personal Communication.

3. Tuttle, M.E. and Brinson, H.F. Resistance-Foil Strain Gauge Technology as Applied to Composite Materials. Experimental Mechanics, March 1984, pp. 54-65.

4. Chang, F.H., Gordon, D.G., and Gardner, A.H. A Study of Fatigue Damage in Composites by Non-Destructive Testing Techniques. Fatigue of Filamentary Composite Materials, Philadelphia, PA: American Society for Testing and Materials, Spec. Tech. Publ. 636, 1977, pp. 57-72.

5. Whitcomb, J.D. Thermographic Measurement of Fatigue Damage. Composite Materials: Testing and Design (Fifth Conference). Philadelphia, PA: American Society for Testing and Materials, Spec. Tech. Publ. 674, 1979, pp. 502-516.

6. Preuss, T.E. Australian Aeronautical Research Laboratories Tech. Memo. in preparation.

7. Watters, K.C., Sparrow, J.G. and Jones, R. Shadow Moire Monitoring of Damaged Graphite/Epoxy Specimens. Aust. Aeronaut. Res. Labs Structures Technical Memorandum 398, 1985.

8. Matondang, T.H., and Schultz, D. The Influence of Anti-Buckling Guides on the Compression Fatigue Behaviour of Carbon Fibre-Reinforced Plastic Laminates. Composites vol. 15, no. 3, July 1984, pp. 217-221.

9. Sarma Avva, V. Impact Initiated Damage in Laminated Composites. School of Engineering, North Carolina A&T State University. Final Report for Air Force Office of Scientific Research, 1982.

10. Roark, R.J., and Young, W.C. Formulas for Stress and Strain. New York: McGraw-Hill, 1975.

11. Cantwell, W.J., and Morton, J. Detection of Impact Damage in CFRP Laminates. Composite Structures, vol. 3, 1985, pp. 241-257.

12. Demuts, E., Whitehead, R.S., and Deo, R.B. Assessment of Damage Tolerance in Composites. Composite Structures, vol. 4, 1985, pp. 45-58.

Fig. 1 Box beam specimen, showing 56-ply $[\pm 45/0_2]_{7S}$ XAS-914C CFC skin attached to metal substructure by means of titanium screws.

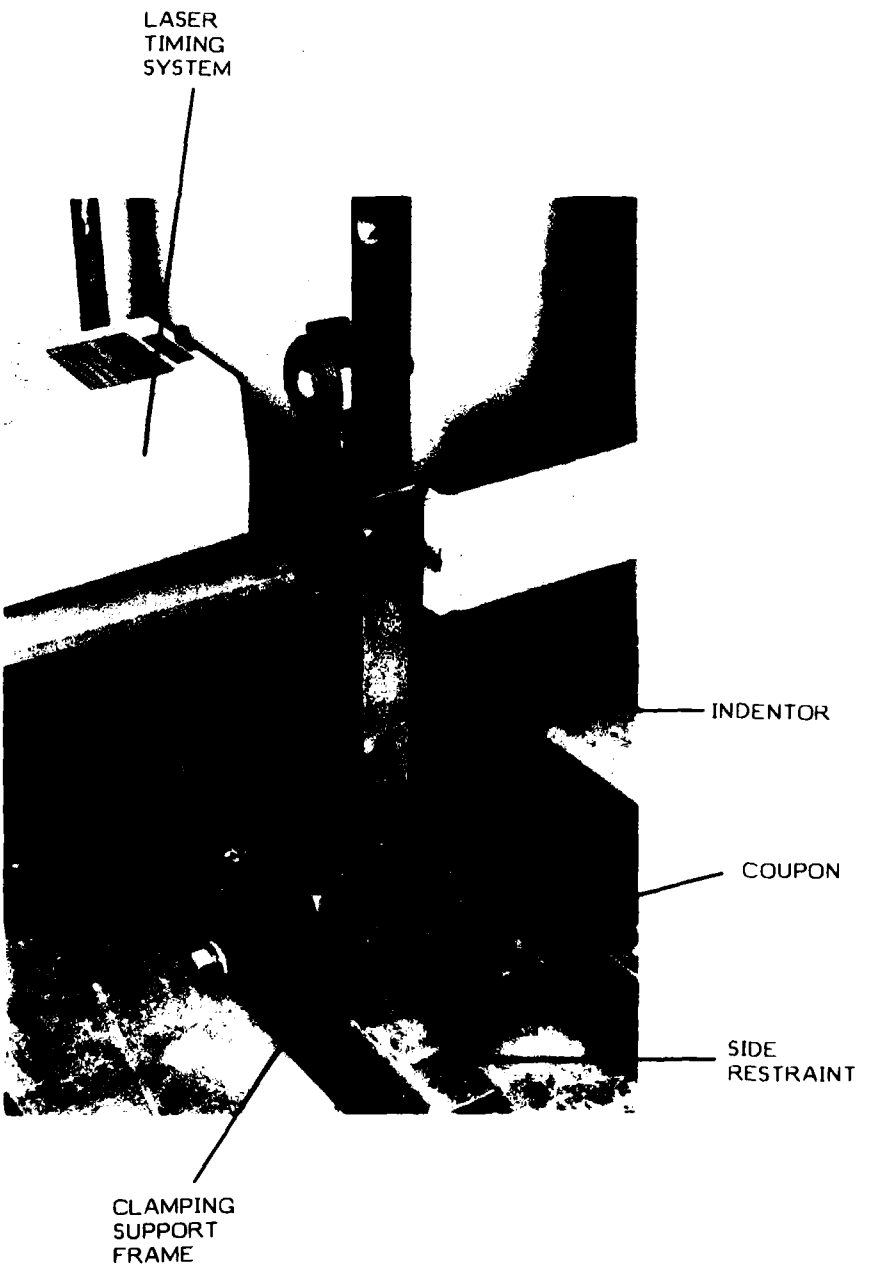

Fig. 2 Falling mass rig used to impact-damage coupons.

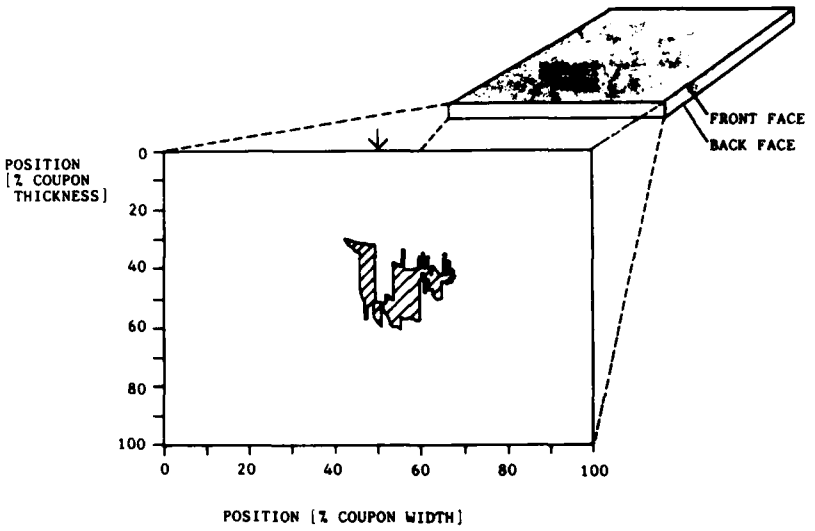

Fig. 3 *Typical impact damage profile for 56-ply coupon, determined by* ultrasonic scanning from both faces of the specimen.

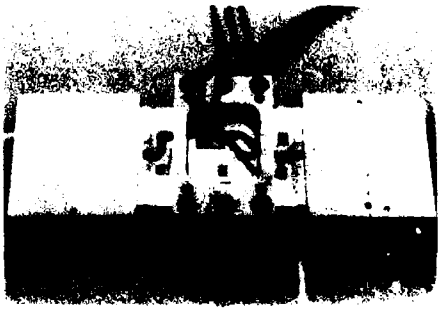

Fig. 4 Experimental antibuckling restraint, showing strain-gauged aluminium alloy dummy specimen used to evaluate restraint performance.

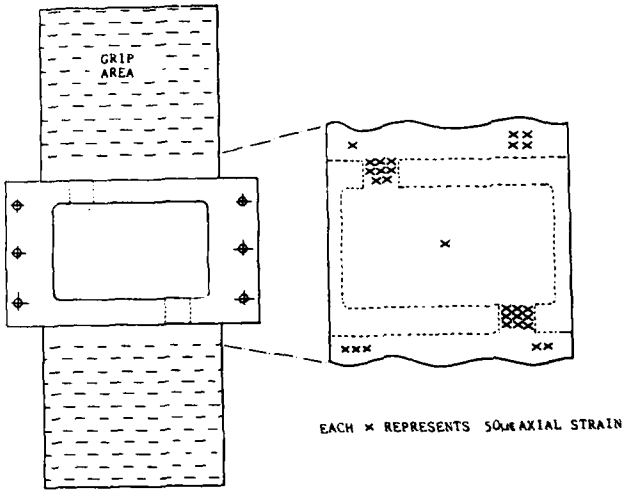

Fig. 5 Experimentally determined strain concentrations resulting from restraint shown in Fig. 4.

Fig. 6 ARL compression test fixture illustrating the three antibuckling restraint systems used for coupon testing. (a) stud support, (b) crossbar support, (c) plates supported by crossbars.

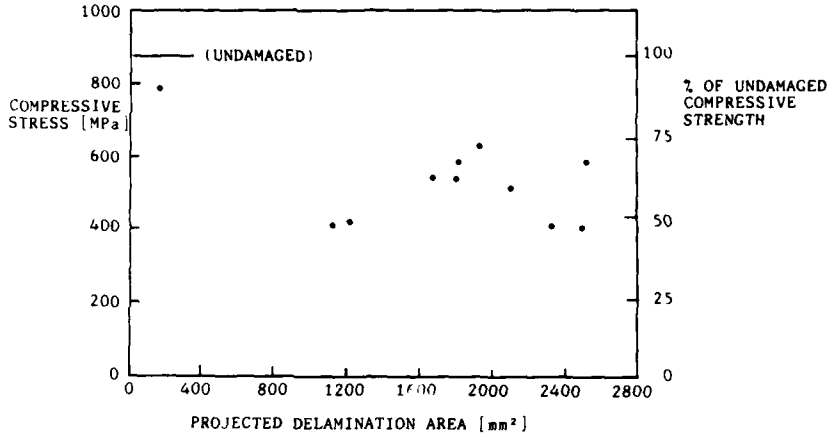

Fig. 7 Residual compressive strength as a function of total projected delamination area for 56-ply coupons.

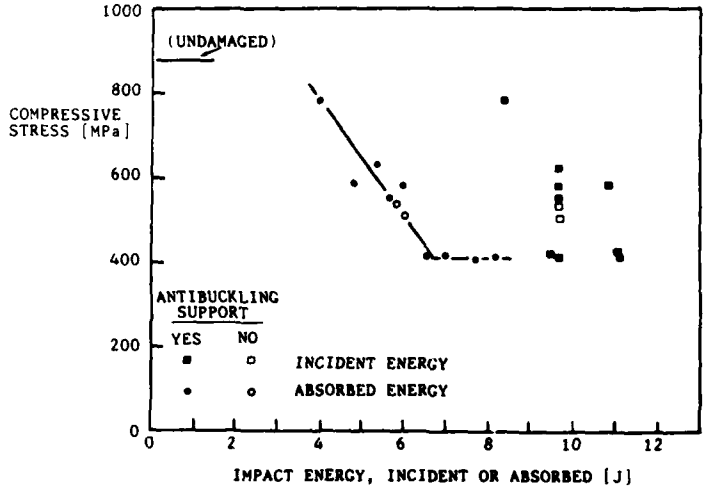

Fig. 8 Residual compressive strength as a function of incident and absorbed energy for impact damaged 56-ply coupons. Open symbols refer to tests conducted without antibuckling restraints.

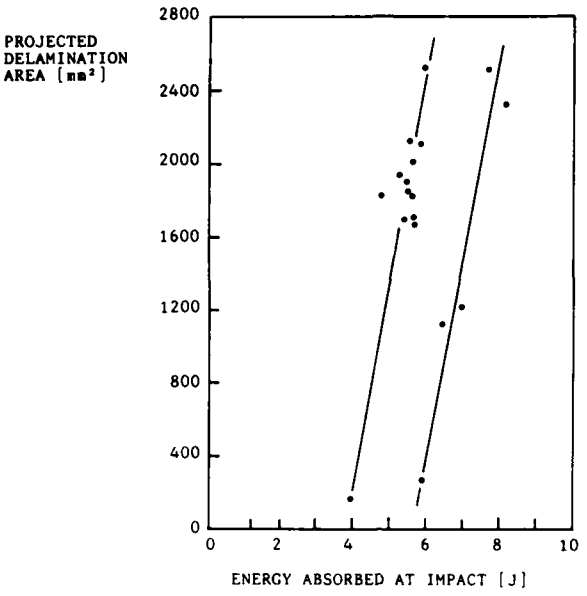

Fig. 9 Projected delamination area produced by impacting 56-ply coupons at different energies.

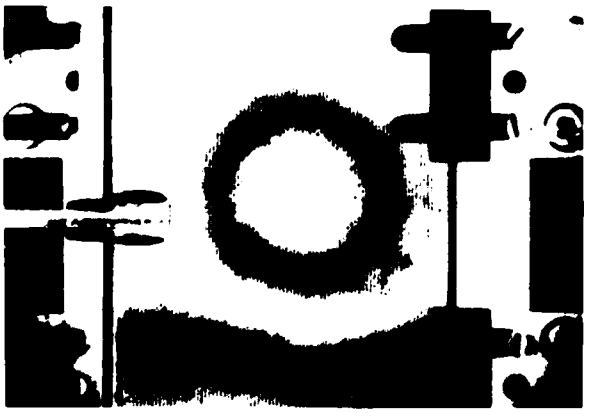

Fig. 10 Out-of-plane displacements (0.15 mm per fringe) for a damaged 56-ply coupon under static compression load.

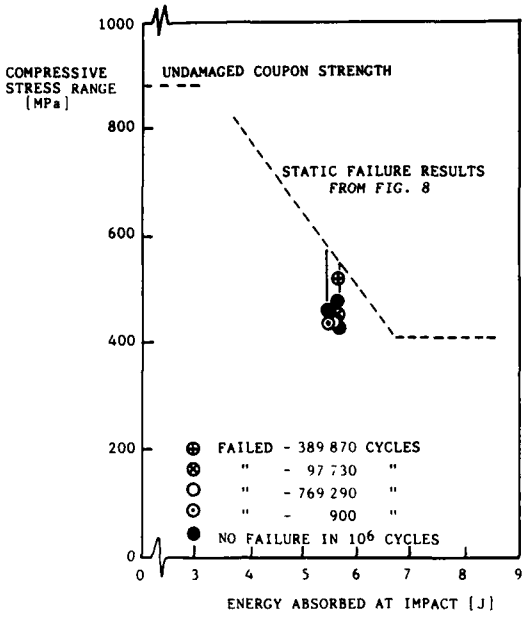

Fig. 11 Fatigue test results (zero to compression) for impact damaged 56-ply coupons.

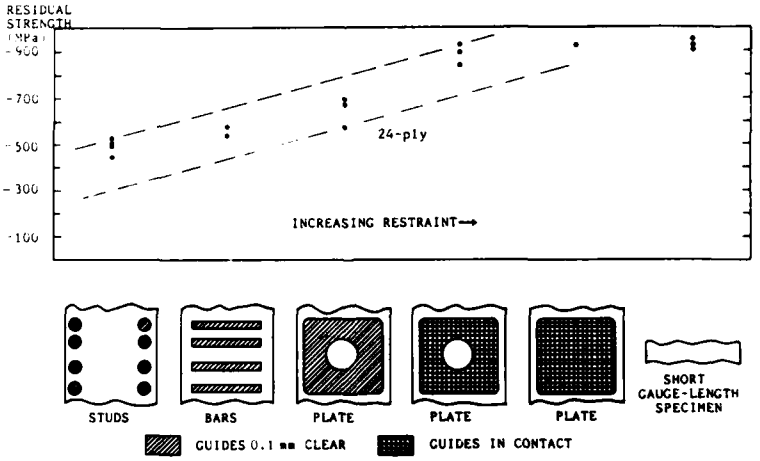

Fig. 12 The effect of increased test rig antibuckling restraint upon the residual compressive strength of undamaged 24-ply coupons.

Fig. 13. Shadow Moire representation of the buckling of an inadequately restrained undamaged 24-ply coupon undergoing static compression testing.

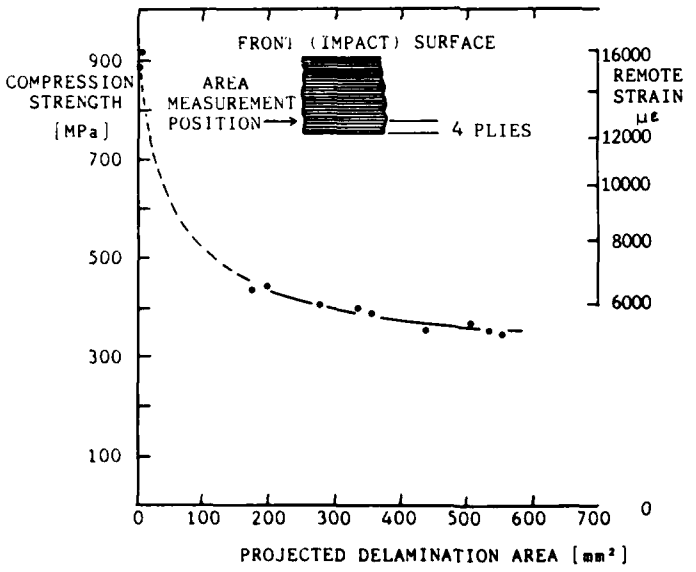

Fig. 14 Residual strength as a function of delamination area for impact-damaged 24-ply coupons. The values of strain shown are measured at points remote from the delamination.

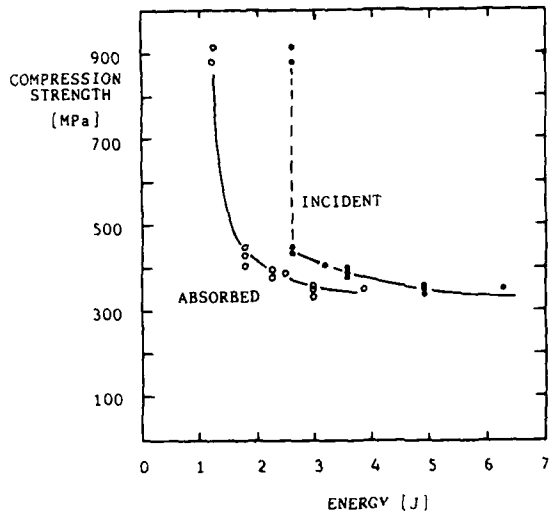

Fig. 15 Residual strength of impact damaged 24-ply coupons as a function of incident and absorbed impact energies.

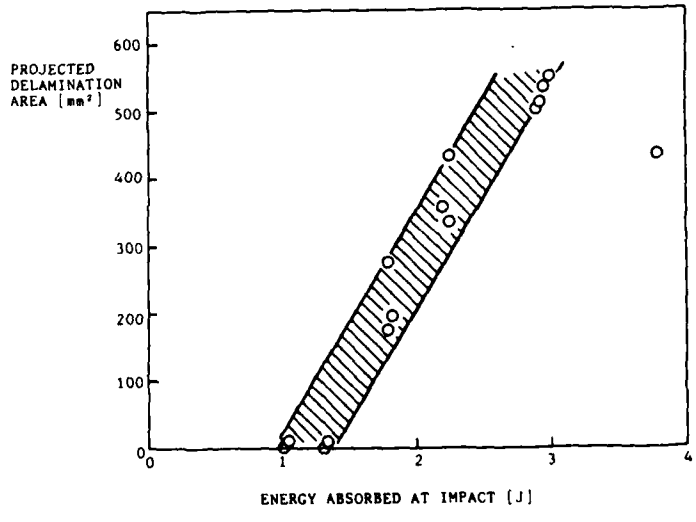

Fig. 16 Delamination area produced by impacting 24-ply coupons at various energy levels.

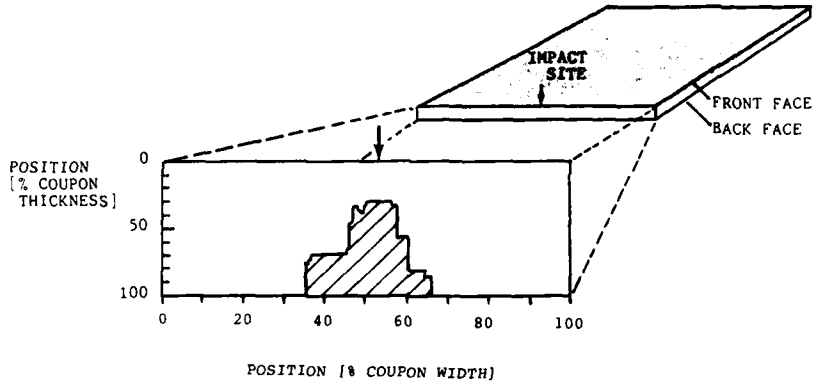

Fig. 17 Typical impact damage profile for 24-ply coupon, determined by ultrasonic scanning.

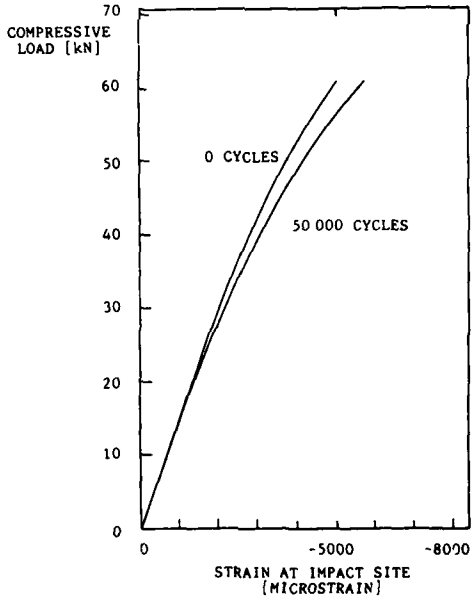

Fig. 18(a) Change in local compliance in the damaged region of a 24-ply coupon after 50 000 cycles of fatigue loading.

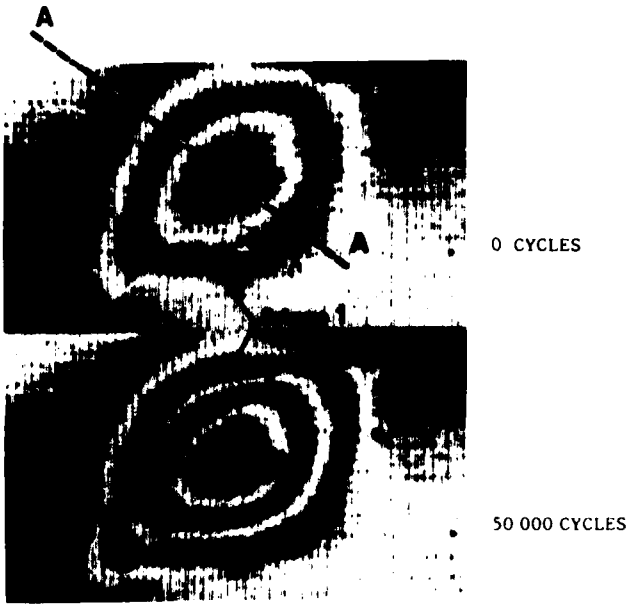

Fig. 18(b) Delamination damage growth in 50 000 fatigue cycles, revealed by enlargement of Moire fringe pattern and by increasing out-of-plane displacements (0.15 mm per fringe).

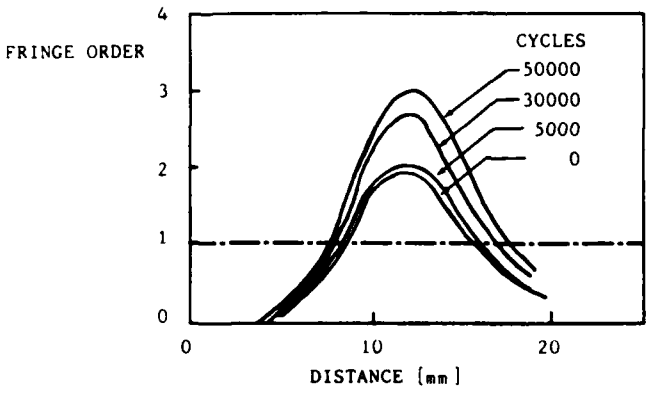

Fig. 18(c) Profile of fringe pattern through section A-A in Fig. 18(b).

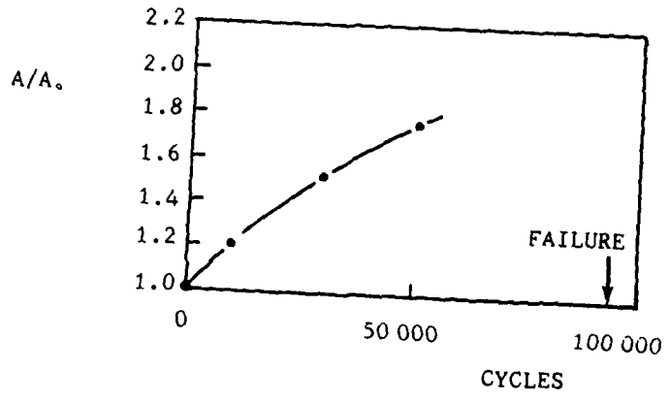

Fig. 18(a) Increase in delamination area (A), relative to initial value (A_0). This ratio was estimated from the changing position of fringe 1 in Figs 18 (b) and (c).

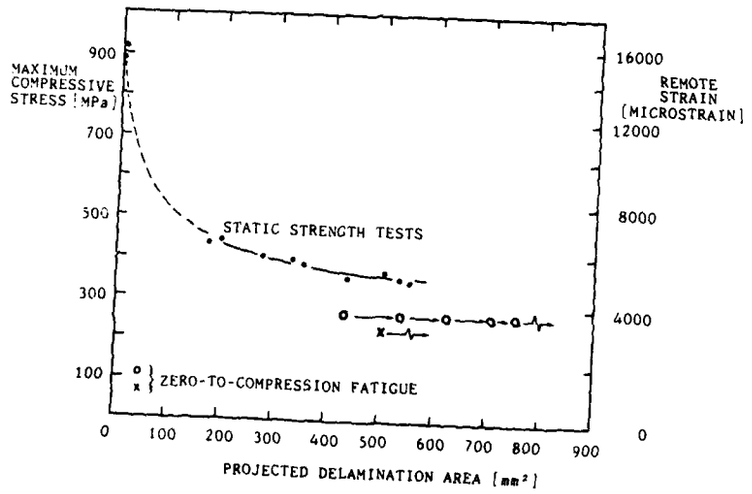

Fig. 19 Growth of delamination in impact damaged 24-ply coupons during zero-to-compression fatigue. Open symbols indicate growth in delamination size at 12 500 cycle increments.

DISTRIBUTION

AUSTRALIA

Department of Defence

Defence Central
- Chief Defence Scientist
- Deputy Chief Defence Scientist (shared copy)
- Superintendent, Science and Program Administration (shared copy)
- Controller, External Relations, Projects and Analytical Studies (shared copy)
- Counsellor, Defence Science (London) (Doc Data Sheet Only)
- Counsellor, Defence Science (Washington) (Doc Data Sheet Only)
- Defence Science Representative (Bangkok)
- Defence Central Library
- Document Exchange Centre, DISB (18 copies)
- Joint Intelligence Organisation
- Librarian H Block, Victoria Barracks, Melbourne
- Director General - Army Development (NSO) (4 copies)

Aeronautical Research Laboratories
- Director
- Library
- Divisional File - Structures
- Authors: G. Clark
  T.J. Van Blaricum
- B.C. Hoskin
- A.A. Baker
- J.M. Finney
- P.W. Beaver
- C.K. Rider
- J.G. Sparrow
- K.C. Watters
- D. Saunders
- R.G. Parker
- R. Jones
- G.S. Jost

Materials Research Laboratories
- Director/Library

Defence Research Centre
- Library

RAN Research Laboratory
- Library

Navy Office
- Navy Scientific Adviser

Army Office
- Scientific Adviser - Army
- Engineering Development Establishment, Library
- Royal Military College Library
- US Army Research, Development and Standardisation Group

Air Force Office
- Air Force Scientific Adviser
- Aircraft Research and Development Unit
  - Scientific Flight Group
  - Library
- Technical Division Library
- Director General Aircraft Engineering - Air Force

Central Studies Establishment
- Information Centre

Government Aircraft Factories
- Manager
- Library

Department of Aviation
- Library
- Flight Standards Division
- Mr C. Torkington

Statutory and State Authorities and Industry
- Australian Atomic Energy Commission, Director
- Australian Airlines, Library
- Qantas Airways Limited
- SEC of Vic., Herman Research Laboratory, Library
- Ansett Airlines of Australia, Library
- BHP, Melbourne Research Laboratories
- Hawker de Havilland Aust Pty Ltd, Bankstown, Library
- Hawker de Havilland Aust Pty Ltd, Victoria, Limited, Library
- Rolls Royce of Australia Pty Ltd, Mr C.G.A. Bailey

Universities and Colleges
- Melbourne
  - Engineering Library
- Monash
  - Hargrave Library
  - Professor I.J. Polmear, Materials Engineering
- Newcastle
  - Library
- Sydney
  - Engineering Library

NSW
Physical Sciences Library
Library, Australian Defence Force Academy

RMIT
Library

CANADA
CAARC Coordinator Structures
International Civil Aviation Organization, Library
NRC
Aeronautical & Mechanical Engineering Library

Universities and Colleges

Toronto
Institute for Aerospace Studies

CZECHOSLOVAKIA
Aeronautical Research and Test Institute (Prague), Head

FRANCE
ONERA, Library

INDIA
CAARC Coordinator Materials
CAARC Coordinator Structures
Defence Ministry, Aero Development Establishment, Library
Hindustan Aeronautics Ltd, Library
National Aeronautical Laboratory, Information Centre

INTERNATIONAL COMMITTEE ON AERONAUTICAL FATIGUE
per Australian ICAF Representative (27 copies)

ISRAEL
Technion-Israel Institute of Technology
Professor J. Singer

JAPAN
National Aerospace Laboratory
Institute of Space and Astronautical Science, Library

NETHERLANDS
National Aerospace Laboratory (NLR), Library

NEW ZEALAND
Defence Scientific Establishment, Library

SWEDEN
Aeronautical Research Institute, Library
Swedish National Defense Research Institute (FOA)

SWITZERLAND

F+W (Swiss Federal Aircraft Factory)

UNITED KINGDOM

Ministry of Defence, Research, Materials and Collaboration
CAARC, Secretary
Royal Aircraft Establishment
Bedford, Library
Farnborough, Dr G. Wood, Materials Department
Commonwealth Air Transport Council Secretariat
National Engineering Laboratory, Library
British Library, Document Supply Centre
CAARC Co-ordinator, Structures
Rolls-Royce Ltd, Aero Division Bristol, Library
British Aerospace
Kingston-upon-Thames, Library
Hatfield-Chester Division, Library

Universities and Colleges

Bristol
Engineering Library

Cambridge
Library, Engineering Department

London
Professor G.J. Hancock, Aero Engineering

Southampton
Library

Strathclyde
Library

Cranfield Inst. of Technology
Library

Imperial College
Aeronautics Library

UNITED STATES OF AMERICA

NASA Scientific and Technical Information Facility
The Chemical Abstracts Service
United Technologies Corporation, Library
Lockheed-California Company
Lockheed Missiles and Space Company
Lockheed Georgia
McDonnell Aircraft Company, Library

Universities and Colleges

Chicago
John Crerar Library

Massachusetts Inst. of Tech.
MIT Libraries

SPARES (20 copies)
TOTAL (172 copies)

Department of Defence

DOCUMENT CONTROL DATA

1.a. AR No	1.b. Establishment No	2. Document Date	3. Task No
AR-004-495	ARL-STRUC-R-422	AUGUST 1986	AIR 80/126

4. Title	5. Security a. document b. title c. abstract	6. No Pages	7. No Refs
CARBON FIBRE COMPOSITE COU. ONS - STATIC AND FATIGUE BEHAVIOUR AFTER IMPACT DAMAGE	UNCLASSIFIED U U	16	12

8. Author(s)	9. Downgrading Instructions
G. CLARK, T.J. VAN BLARICUM	

10. Corporate Author and Address	11. Authority (as appropriate) a.Sponsor b.Security c.Downgrading d.Approval
Aeronautical Research Laboratories P.O. Box 4331, MELBOURNE, VIC. 3001	

12. Secondary Distribution (of this document)

Approved for public release.

Overseas enquirers outside stated limitations should be referred through ASDIS, Defence Information Services Branch, Department of Defence, Campbell Park, CANBERRA ACT 2601

13.a. This document may be ANNOUNCED in catalogues and awareness services available to ...

No limitations

13.b. Citation for other purposes (ie. casual announcement) may be unrestricted

14. Descriptions		15. COSATI Group
Graphite epoxy composites	Delamination	1104
Fatigue	Impact damage	
Residual strength		
Coupon specimens		

16. Abstract

This report describes some results from an experimental program involving the determination of static and fatigue properties of relatively thick (3 to 7 mm) carbon fibre composite laminates which had been subjected to various levels of impact damage. The development of suitable compression testing procedures is described as is the use of shadow Moire interference techniques for monitoring the development of delamination damage during fatigue tests.

PF 35

This paper is to be used to record information which is required by the Establishment for its own use but which will not be added to the DISTIS data base unless specifically requested.

16. Abstract (contd)

17. Imprint

Aeronautical Research Laboratories, Melbourne

18. Document Series and Number	19. Cost Code	20. Type of Report and Period Covered
Structures Report 422	21 4655	

21. Computer Programs Used

22. Establishment File Ref(s)

END

DATE
FILMED
5-87

DTIC